Please note:

If you experience some difficulty in viewing some of the pages, use the magnifying tool to enlarge the specific section

UCRL- 92424
PREPRINT

Dynamic ADI Computations of Thermoelastic Stresses in Crystalline Laser Media

R. J. Gelinas
S. K. Doss
N. N. Carlson

This paper was prepared for submittal to:
Fourth International Conference on Numerical Methods in Thermal Problems, Swansea, UK
July 15-18, 1985

April 1, 1985

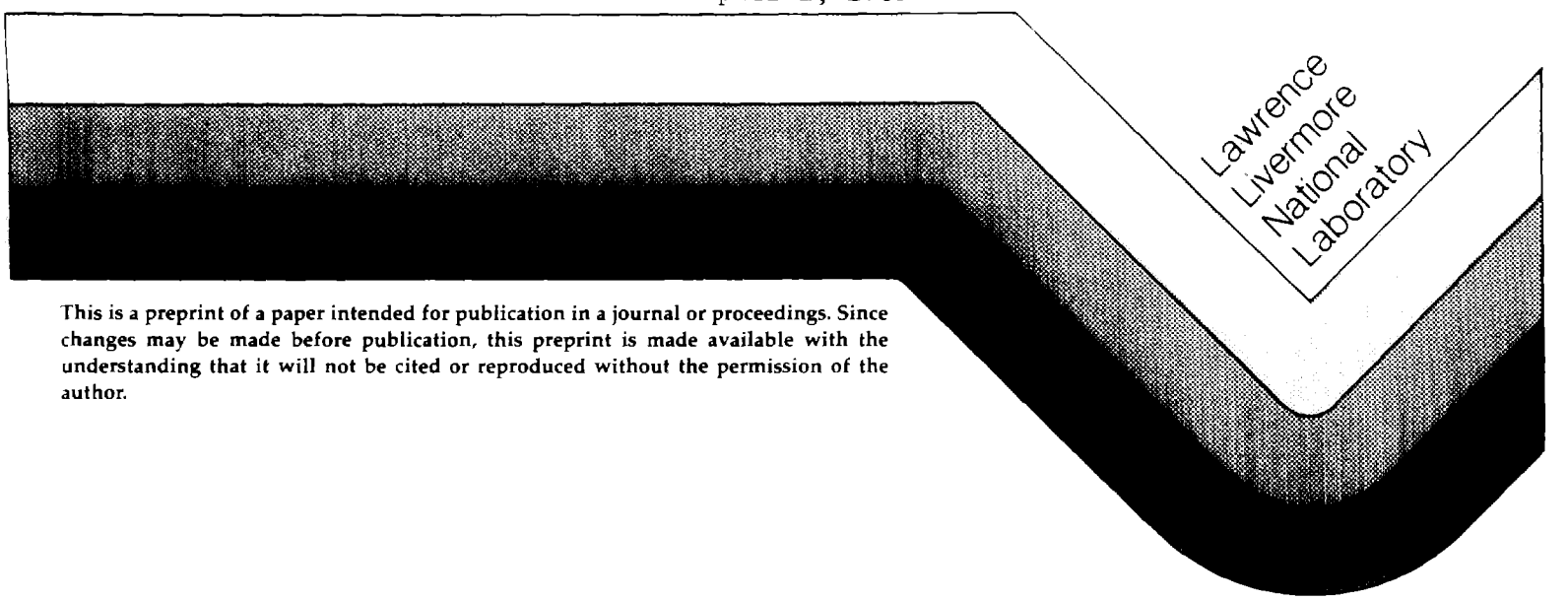

DYNAMIC ADI COMPUTATIONS OF THERMOELASTIC STRESSES IN CRYSTALLINE LASER MEDIA*

R. J. Gelinas, S. K. Doss, N. N. Carlson+
Lawrence Livermore National Laboratory
Livermore, California, 94550 USA

+University of California, Berkeley, California, USA

SUMMARY. This article considers thermoelastic effects which influence both the thermal engineering design and optical propagation in solid state high average power laser (HAPL) systems. The methods and computations described here have been developed for applications, ultimately, to crystalline slabs with arbitrary symmetry properties and with arbitrary spatial orientations between crystalline axes and slab configurations. For this, accurate numerical solutions are required simultaneously for the heat equation and Hooke's law in their most general tensor forms.

Prompted by the optical problem requirements in HAPL systems, this work utilizes new implementations of Eulerian discretizations and dynamic ADI methods for solving general fourth-order elliptic partial differential equations (PDE's) which describe stress potentials in anisotropic media. These formulations can provide both steady state and transient PDE solutions. This article concludes with computed results for trigonal Al_2O_3 crystal deformations in various crystal axes/slab orientations.

1. INTRODUCTION. Thermoelastic stress analysis comes to bear in at least two major areas of solid state high average power laser (HAPL) design. The first area is in the thermal engineering and physics analysis of coolant flows, materials selection, system configuration, etc. The second area is in optical propagation analysis where stress induced birefringence and thermal lensing effects are potentially significant factors in (HAPL) beam quality. These latter factors of beam quality govern the computational and physics approaches which are applied in this work. A typical problem can be sketched, for example, by noting that relatively low thermal conductivities of doped laser glasses permit thermal peaks to build up within the glass when flashlamp radiation is absorbed. Such thermal

*This work was performed under the auspices of the U.S. Department of Energy by Lawrence Livermore National Laboratory under contract No. W-7405-Eng-48.

peaks can generate thermal stresses which approach tensile yield strengths at only modest average power levels ($O(10^2-10^3 W)$) [1]. These peaks can also generate stress-induced birefringence and thermal lensing effects which may adversely affect beam polarization and phase properties. Several possible measures are taken to address these problems. First, freely-suspended laser slabs are used in order to eliminate mechanically induced stresses. Second, we consider only small material deformations; laser slabs with large material displacements are--by definition--poor designs. Third, various candidate crystals for high average power lasers are known to have thermal conductivities which exceed those of laser glasses by wide margins. But crystal symmetries have their own principal frames of reference, in addition to the principal stress orientations. These geometrical factors act to complicate the analysis of thermal stress-induced birefringence in slabs which are cut in arbitrary shapes and orientations relative to crystal axes and to flashlamp pump source functions.

In order to accommodate these various specific problems in HAPL designs, the TECATE code has been formulated, validated, and applied to numerous practical problems. This article presents the basic physics formulations and some selected sample problem results.

2. PHYSICS FORMULATIONS. Figure 1 shows schematically a simple slab amplifier test assembly which is being used in early baseline evaluations. The Nd-doped glass is used for purposes of calibrations and code validations; candidate laser crystals will replace the glass slab in later applications. We focus our attention upon the rectangular slab cross section which is practically freely suspended by the soft elastomer mounting, as shown in Fig. 1.

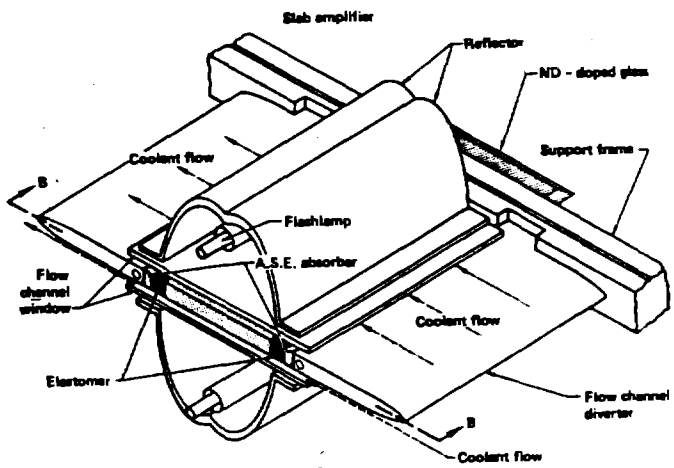

Fig. 1. A simple slab amplifier system.

2.1 Heat Flow in Anisotropic Media

The time-dependent heat equation for a crystalline slab is written as

$$\rho c \frac{\partial T}{\partial t} = \nabla \cdot (\mathbf{K} \cdot \nabla T) + Q, \tag{1}$$

where

- $T \equiv$ temperature (degrees)
- $\rho \equiv$ mass density (mass/volume)
- $c \equiv$ heat capacity (energy/mass-degree)
- $\mathbf{K} \equiv$ symmetric thermal conductivity tensor (power/length-degree)
- $Q \equiv$ rate of internal heat generation (power/volume)

It is presently assumed that ρ, c, and the components of the tensor $\mathbf{K}$ are all constants; this restriction can readily be relaxed, as in Reference 2. In the majority of our work the source function Q and the boundary conditions are independent of time, which permits steady-state solutions to exist and to be obtained from the PDE

$$\nabla \cdot (\mathbf{K} \cdot \nabla T) = -Q. \tag{2}$$

We further consider numerous problems in which the Z-dependence can be discarded. In such physical circumstances the 2-D equation,

$$\nabla \cdot (\mathbf{K}^* \cdot \nabla T) \equiv k_{11} \frac{\partial^2 T}{\partial x^2} + 2k_{12} \frac{\partial^2 T}{\partial x \partial y} + k_{22} \frac{\partial^2 T}{\partial y^2} = -Q, \tag{3}$$

represents rigorously the 3-D physical system subject to Dirichlet, natural Neumann, and film boundary conditions. It is assumed that $k_{11} k_{22} > k_{12}^2$ (i.e. $\mathbf{K}^*$ is positive definite). Eqn. (3) is thus elliptic, and solution by the alternating directions implicit (ADI) method is quite appropriate.

The slab geometry which is considered in the coupled heat and stress calculations of the TECATE code is shown in Fig. 2.

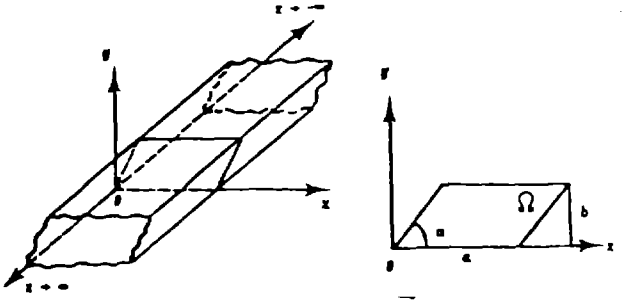

Fig. 2. Slab geometry in the TECATE code.

Both the heat and stress equations are solved by mapping the x-y plane onto the ξ-η plane so that the parallellogram Ω is mapped onto the unit square. The transformed heat equation is then solved according to difference equations which have been derived by integration of the partial differential heat equation on auxiliary cells for both interior grid points (or nodes) and for boundary nodes. The leading truncation error terms have been derived for these difference equations in Ref. 3; and local truncation errors can thus be controlled readily via the number of grid cells which are selected in any given problem by the code user.

2.2 Stress Potential Equations for Thermoelasticity in Anisotropic Media. Stress-optics analyses require accurate evaluations of the full stress tensor σ; and thermal lensing analyses require accurate material displacement values. We follow closely the conventions and notations which have been used by Nye [4]. The symmetric second-rank stress tensor is written alternatively in matrix notation as

$$\sigma = \begin{pmatrix} \sigma_{11} & \sigma_{12} & \sigma_{13} \\ \sigma_{21} & \sigma_{22} & \sigma_{23} \\ \sigma_{31} & \sigma_{32} & \sigma_{33} \end{pmatrix} = \begin{pmatrix} \sigma_{xx} & \sigma_{xy} & \sigma_{xz} \\ \sigma_{yx} & \sigma_{yy} & \sigma_{yz} \\ \sigma_{zx} & \sigma_{zy} & \sigma_{zz} \end{pmatrix} = \begin{pmatrix} \sigma_1 & \sigma_6 & \sigma_5 \\ \sigma_6 & \sigma_2 & \sigma_4 \\ \sigma_5 & \sigma_4 & \sigma_3 \end{pmatrix} \qquad (4)$$

and in the compact notation of a six-component vector

$$\sigma' = (\sigma_1, \sigma_2, \sigma_3, \sigma_4, \sigma_5, \sigma_6)^t. \qquad (5)$$

Generalized Hooke's Law:

For small deformations the stress-strain relationship is given in compact notation by

$$\varepsilon' = S \cdot \sigma' + \alpha' T, \qquad (6)$$

where S is the so-called compliance matrix, $S = (s_{ij})$, and T here represents the temperature deviation from that of the undeformed state. The strain-displacement relationships are:

$$\varepsilon_1 = \frac{\partial u}{\partial x} \qquad \varepsilon_4 = \frac{\partial v}{\partial z} + \frac{\partial w}{\partial y}$$

$$\varepsilon_2 = \frac{\partial v}{\partial y} \qquad \varepsilon_5 = \frac{\partial u}{\partial z} + \frac{\partial w}{\partial x} \qquad (7)$$

$$\varepsilon_3 = \frac{\partial w}{\partial z} \qquad \varepsilon_6 = \frac{\partial u}{\partial y} + \frac{\partial v}{\partial x}$$

where the material displacements are denoted by $d = (u, v, w)t$.

With these definitions and conventions, PDE's can now be developed for the stress potentials. The general 3-D balance of force equation with zero external body forces is $\nabla \cdot \sigma = 0$. In expanded form

$$\begin{aligned} \frac{\partial \sigma_1}{\partial x} + \frac{\partial \sigma_6}{\partial y} + \frac{\partial \sigma_5}{\partial z} &= 0 , \\ \frac{\partial \sigma_6}{\partial x} + \frac{\partial \sigma_2}{\partial y} + \frac{\partial \sigma_4}{\partial z} &= 0 , \\ \frac{\partial \sigma_5}{\partial x} + \frac{\partial \sigma_4}{\partial y} + \frac{\partial \sigma_3}{\partial z} &= 0 . \end{aligned} \tag{8}$$

It is plausible to conclude from the assumptions made in the heat problem classification above that all stresses are independent of the z-coordinate, and by Hooke's Law the strains are also independent of z. The displacement vector can also be shown to be independent of z. Geometrically, this implies that the planar domain Ω would in general deform to a non-planar surface. Such deformations will be referred to as generalized plane deformations. The system of equations (8) thus reduces to

$$\begin{aligned} \frac{\partial \sigma_1}{\partial x} + \frac{\partial \sigma_6}{\partial y} &= 0 , \\ \frac{\partial \sigma_6}{\partial x} + \frac{\partial \sigma_2}{\partial y} &= 0 , \\ \frac{\partial \sigma_5}{\partial x} + \frac{\partial \sigma_4}{\partial y} &= 0 . \end{aligned} \tag{9}$$

Equation (9) will frequently be referred to as the reduced set of balance of force equations. The PDE system (9) consists of three equations in the five unknowns σ_1, σ_2, σ_4, σ_5, and σ_6. Two more equations are needed in order to determine a unique solution. These extra equations are the so-called compatibility equations. Invoking the fact that the displacement vector d is independent of z in Eqn. (7), it follows that the strains can be defined simply as

$$\begin{aligned} \varepsilon_1 &= \frac{\partial u}{\partial x} \quad \varepsilon_2 = \frac{\partial v}{\partial y} \quad \varepsilon_3 = 0, \\ \varepsilon_4 &= \frac{\partial w}{\partial x} \quad \varepsilon_5 = \frac{\partial w}{\partial y} \quad \varepsilon_6 = \frac{\partial v}{\partial x} + \frac{\partial u}{\partial y} , \end{aligned} \tag{10}$$

and that the following compatibility relationships hold:

$$\frac{\partial^2 \varepsilon_1}{\partial y^2} - \frac{\partial^2 \varepsilon_6}{\partial x \partial y} + \frac{\partial^2 \varepsilon_2}{\partial x^2} = 0 , \tag{11a}$$

$$\frac{\partial \epsilon_4}{\partial x} - \frac{\partial \epsilon_5}{\partial y} = 0 \quad . \tag{11b}$$

By the use of Hooke's Law in Eqns. (11), one obtains together with Eqn. (9) a system of five PDE's in σ_1, σ_2, σ_4, σ_5, σ_6 of maximum order two. From here PDE's can be developed for stress potentials. The basic logic is as follows:

(i) Stresses are defined as some linear combinations of certain derivatives of potential functions.
(ii) In terms of these potentials the balance of force equations should be satisfied identically.
(iii) The number of potentials is equal to the smallest possible number of compatibility equations.
(iv) These potentials are solutions to the compatibility equations.

In general, these stress potentials are not unique. (See Reference 4). In addition to the above criteria, one attempts to choose those potentials which contain certain desirable characteristics. For example, the potential functions chosen below use the positive definite property of potential energy to show that they are solutions of elliptic systems of PDE's [3] and that a dynamic alternating direction implicit (DADI) method can thus be used to solve both the heat and stress potential equations with high levels of numerical efficiency.

The Potential Equations:

i. For the general balance of force Eqn (8), the three potentials ϕ, ψ, and χ are introduced such that

$$\sigma_1 = \frac{\partial^2 \chi}{\partial y^2} + \frac{\partial^2 \psi}{\partial z^2} \qquad \sigma_4 = -\frac{\partial^2 \phi}{\partial y \partial z}$$

$$\sigma_2 = \frac{\partial^2 \phi}{\partial z^2} + \frac{\partial^2 \chi}{\partial x^2} \qquad \sigma_5 = -\frac{\partial^2 \psi}{\partial z \partial x} \tag{12}$$

$$\sigma_3 = \frac{\partial^2 \psi}{\partial x^2} + \frac{\partial^2 \phi}{\partial y^2} \qquad \sigma_6 = -\frac{\partial^2 \chi}{\partial x \partial y} \quad .$$

ii. For the reduced balance of force equations, only two potentials ϕ and ψ are needed, such that

$$\sigma_1 = \frac{\partial^2 \phi}{\partial y^2} \qquad \sigma_2 = \frac{\partial^2 \phi}{\partial x^2} \qquad \sigma_6 = -\frac{\partial^2 \phi}{\partial x \partial y}$$

$$\sigma_5 = \frac{\partial \psi}{\partial y} \qquad \sigma_4 = -\frac{\partial \psi}{\partial x} \quad . \tag{13}$$

It can readily be shown that Eqns (12) and (13) meet the criteria mentioned above. Finally, using Hooke's Law in Eqn (11) and Eqn (13), the following system of PDE's is obtained for the potentials ϕ and ψ:

$$L_4\phi + L_3\psi = M_2T, \tag{14a}$$

$$L_2\psi + L_3\phi = M_1T, \tag{14b}$$

where

$$L_4 = s'_{22}\frac{\partial^4}{\partial x^4} - 2s'_{26}\frac{\partial^4}{\partial x^3\partial y} + (2s'_{12}+s'_{66})\frac{\partial^4}{\partial x^2\partial y^2} - 2s'_{16}\frac{\partial^4}{\partial x\partial y^3} + s'_{11}\frac{\partial^4}{\partial y^4},$$

$$L_3 = s'_{24}\frac{\partial^3}{\partial x^3} + (s'_{25}+s'_{46})\frac{\partial^3}{\partial x^2\partial y} - (s'_{14}+s'_{56})\frac{\partial^3}{\partial x\partial y^2} + s'_{15}\frac{\partial^3}{\partial y^3},$$

$$L_2 = s'_{44}\frac{\partial^2}{\partial x^2} - 2s'_{45}\frac{\partial^2}{\partial x\partial y} + s'_{55}\frac{\partial^2}{\partial y^2}, \tag{15}$$

$$M_2 = -\alpha'_2\frac{\partial^2}{\partial x^2} + \alpha'_6\frac{\partial^2}{\partial x\partial y} - \alpha'_1\frac{\partial^2}{\partial y^2},$$

$$M_1 = \alpha'_4\frac{\partial}{\partial x} - \alpha'_5\frac{\partial}{\partial y}.$$

The terms s'_{ij} are expressed in terms of the compliance matrix elements s_{ij} by the relationship

$$s'_{ij} = s_{ij} - \frac{s_{i3}s_{3j}}{s_{33}}, \tag{16}$$

and α'_i is expressed in terms of α_i by the relation

$$\alpha'_i = \alpha_i - \alpha_3\frac{s_{i3}}{s_{33}}. \tag{17}$$

The PDE's (14) are mapped onto the unit square and discretized into difference equations by the same methods which were used previously for the heat equation. The formulations of these discretizations for fourth-order equations is lengthy and the reader is referred to Reference 3 for fully detailed descriptions. Free-surface boundary conditions are applied, and these stress potential equations are solved numerically for

stresses and also for the derived quantities of strains and material displacements. **We call attention to the fact that 3-D stresses σ_1, σ_2, σ_3, σ_4, σ_5, σ_6 and 3-D displacements u, v, w are computed rigorously from the theory which includes explicitly only the two independent spatial variables x and y, subject to the assumed independence of temperature loadings upon z for slabs which are practically infinite in the z-direction.** According to this development the material displacements w in the z-direction can be non-trivial functions of the independent variables x and y--but not of z.

In the special case of plane strain ($\epsilon_3=0$) in isotropic media, only one potential ϕ is needed; and it can be shown that Eqns. (14) reduce identically to the familiar biharmonic equation

$$\frac{1-\nu^2}{E}\left(\frac{\partial^4\phi}{\partial x^4} + 2\frac{\partial^4\phi}{\partial x^2\partial y^2} + \frac{\partial^4\phi}{\partial y^4}\right) = -\alpha(1+\nu)\left(\frac{\partial^2 T}{\partial x^2} + \frac{\partial^2 T}{\partial y^2}\right) . \qquad (18)$$

The TECATE code has been validated extensively against other heat and stress codes [6] [7] at LLNL for isotropic problems.

3. THE DADI METHOD. The noteworthy advance of DADI methods beyond conventional ADI methods was the development of strategies which automatically determine changes in the stepsize Δt dynamically. This dynamic procedure permits Δt to always remain within regions of rapid convergence and to suppress instabilities before they have grown too much. These DADI procedures also minimize the overwhelming array of choices for Δt in standard ADI methods. In order to sketch the development of our DADI method, we define the steady-state solution of the heat and stress potential equations by u and define the n^{th} error by

$$e^n = u - u^n \qquad (19)$$

It can be shown for the PDE, Lu=f, where L=A+B, that

$$e^{n+2} = ((1 + \Delta tA)(1 + \Delta tB))^{-1} ((1 - \Delta tA)(1 - \Delta tB))e^n . \qquad (20)$$

Assuming that e^n is an eigenvector for A and hence B with eigenvalues $-\lambda$ and $-\mu$, respectively, it follows from Eqn. (20) that the reduction factor R for a single double sweep is given by

$$e^{n+2} = \left(\frac{1 - \lambda\Delta t}{1 + \lambda\Delta t}\right)\left(\frac{1 - \mu\Delta t}{1 + \mu\Delta t}\right) e^n \equiv R(\lambda\Delta t, \mu\Delta t)e^n . \qquad (21)$$

Starting from step n + 2 and performing another double sweep, one then obtains u^{n+4}; and the error is $e^{n+4} = u^{n+4} - u$. The convergence factor CF for two double sweeps thus becomes

$$CF = \frac{\| e^{n+4} \|}{\| e^{n} \|} \equiv R^2(\lambda\Delta t, \mu\Delta t) \ . \tag{22}$$

In order to devise a strategy for DADI, we back up to the n^{th} step and perform one giant double sweep with stepsize $2\Delta t$. This double sweep generates the value u^{n+4} and the error $e^{n+4}=u^{n+4}-u$. The test parameter TP is an estimate of the relative local truncation error; it is defined by

$$TP = \frac{\| u^{n+4} - \tilde{u}^{n+4} \|}{\| u^{n+4} - u^{n} \|} = \frac{\| e^{n+4} - \tilde{e}^{n+4} \|}{\| e^{n+4} - e^{n} \|} \ . \tag{23}$$

By use of Eqn. (21) the test parameter can also be written as

$$TP = \left| \frac{R^2(\lambda\Delta t, \mu\Delta t) - R(2\lambda\Delta t, 2\mu\Delta t)}{R^2(\lambda\Delta t, \mu\Delta t) - 1} \right| \ . \tag{24}$$

We consider now the elliptic heat equation in the form

$$L_2 u \equiv a_{20}u_{xx} + 2a_{11}u_{xy} + a_{02}u_{yy} = f \ , \tag{25}$$

and the elliptic fourth-order biharmonic equation

$$L_4 u \equiv u_{xxxx} + 2u_{xxyy} + u_{yyyy} = f \ . \tag{26}$$

The finite difference approximation to (25) can be written as

$$L_2 U \equiv (A_2 + B_2 + C_2)U = F \ , \tag{27}$$

where A_2, B_2, and C_2 correspond essentially to the discretization of u_{xx}, u_{yy}, and u_{xy}, respectively. Similarly for the biharmonic equation, we obtain

$$L_4 U \equiv (A_4 + B_4 + C_4)U = F \ , \tag{28}$$

where A_4, B_4, and C_4 correspond essentially to the discretization of u_{xxxx}, u_{yyyy}, and u_{xxyy}, respectively.

An ADI type double sweep for solving Eqn. (27) is defined by:

$$\begin{aligned} \frac{U^{n+1} - U^{n}}{\Delta t} &= A_2 U^{n+1} + B_2 U^{n} + C_2 U^{n} - F \ , \\ \frac{U^{n+2} - U^{n+1}}{\Delta t} &= A_2 U^{n+1} + B_2 U^{n+2} + C_2 U^{n} - F \ . \end{aligned} \tag{29}$$

Similarly, an ADI type double sweep for Eqn. (28) is defined by

$$\frac{U^{n+1} - U^n}{\Delta t} = -(A_4 U^{n+1} + B_4 U^n + C_4 U^n - F),$$

$$\frac{U^{n+2} - U^{n+1}}{\Delta t} = -(A_4 U^{n+1} + B_4 U^{n+2} + C_4 U^n - F). \tag{30}$$

Notice that the minus sign in Eqn. (30) is required because A_4 and B_4 are positive definite. These DADI integration schemes have been shown to be unconditionally stable [3].

4. COMPUTATIONAL RESULTS. We consider in this example thermoelastic stresses and displacements in a trigonal crystal of Al_2O_3. The orientation of the crystalline axes a and c relative to the orthogonal axes (x_1, x_2, x_3) is defined according to the arbitrarily established conventions which appear in the I.R.E. Standards on Piezoelectric Crystals [8]. Ssee Fig. 3. Material property data for k_{ij}, α_{ij} and for elastic compliances S are defined in this conventional frame of orthogonal axes (x_1, x_2, x_3). Of course, if crystals are cut in shapes and orientations which do not conform or otherwise coincide with (x_1, x_2, x_3), the material property tensors must be transformed appropriately from (x_1, x_2, x_3) to that laboratory frame (x,y,z) which is used in conjunction with the crystal's shape and orientation. These coordinate transformations are described elsewhere in the literature [3] [4], and their practical effects on material deformations are shown in the results below.

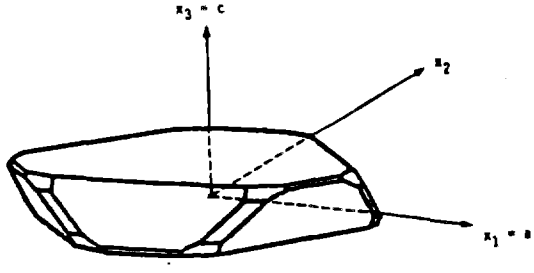

Fig. 3. Conventional coordinate axis orientations for the trigonal crystal Al_2O_3, as defined by IRE Standards.

The trigonal Al_2O_3 crystal in this example is cut in the shape of a rectangular parallelopiped which has a 1 cm square cross-section in the x-y plane and which is practically infinite with uniform temperature loading in the z direction. The temperature deviation function is $\delta T = 4y(1-y) - 2/3$ in all cases considered here. (In other examples we obtain $\delta T(x,y)$ by solving the heat equation with flashlamp pump source functions which deposit heat in the slab according to radiative transport models for absorption of radiation by the slab subject to various

thermal boundary conditions. These flashlamp source descriptions are too lengthy for inclusion in the present article.) In the first case, the slab edges and the laboratory coordinate axes are parallel to the crystal convention axes, as shown in Fig. 4. The material deformation components along (x,y,z) are denoted by (u,v,w). The displacements w in the z-direction are clearly a non-trivial function of x and y. Figure 5 presents case 2 in which the crystal axes orientation is rotated by 90° about the z-axis relative to case 1 above. Finally, the Al_2O_3 crystal can be rotated by 90° about the y-axis relative to case 2 above prior to cutting it into the rectangular slab. (This is now a double rotation relative to the initial orientation which was considered in case 1, Fig. 4.) As can be seen in Fig. 6, the material deformations are now a perfectly planar surface in this final (doubly rotated) orientation.

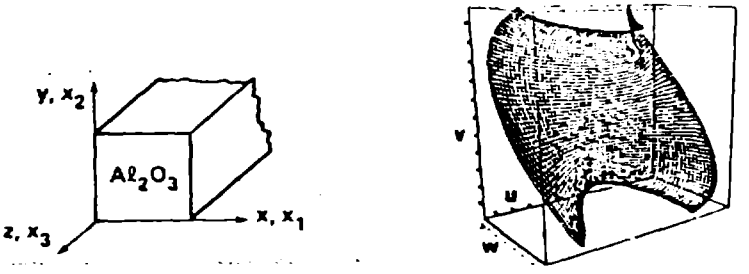

Fig. 4. Magnified deformation of Al_2O_3 slab in conventional frame; Case 1.

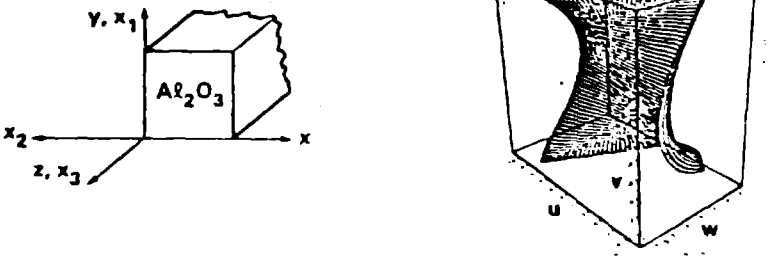

Fig. 5. Case 2: Deformed Al_2O_3 slab with crystal axes rotated by 90° about Z-axis relative to Case 1.

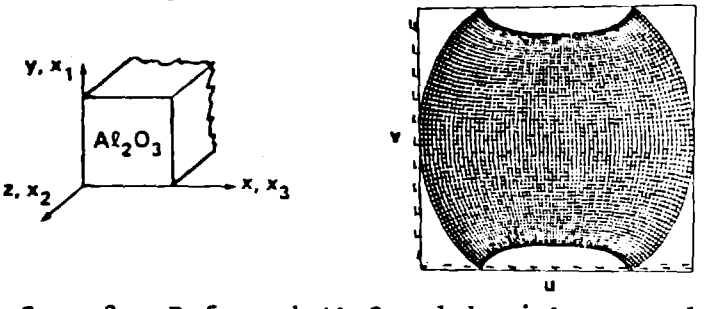

Fig. 6. Case 3: Deformed Al_2O_3 slab with crystal axes rotated by 90° about Y-axis relative to Case 2.

All of the TECATE solutions in this example converged in fewer than 30 DADI iterations, and the CPU time on the LLNL CRAY IS computer was a fraction of a second for the largest mesh considered (81x51).

5. CONCLUSIONS. The DADI method has been applied in the TECATE code to obtain numerical solutions of both the heat equation and an elliptic system of fourth-order PDE's for stress potentials which describe thermoelasticity in arbitrary symmetry classes and thermal environments for freely suspended crystalline slabs. Local truncation error properties of those discretization schemes which are used in TECATE have been derived theoretically and confirmed experimentally for temperatures, for stress potentials, and for the derived material stresses, strains, and displacements. Although this work has been limited at the present time to the study of two-dimensional equations, this approach, with proper generalizations, can be applied to treat also the case of finite crystalline slabs with three-dimensional equations.

References

1. J. L. Emmett, W. F. Krupke, and J. B. Trenholme, "The Future Development of High Power Solid State Laser Systems", Physics of Laser Fusion, Vol. IV, Lawrence Livermore National Laboratory, UCRL-53344 (1982).
2. S. K. Doss, "Dynamic ADI Methods for Elliptic Equations with Gradient Dependent Coefficients", Ph.D. Thesis, LBL-6142 (1977).
3. S. K. Doss, N. N. Carlson, R. J. Gelinas, "Finite Difference Solutions of Thermoelasticity in Anisotropic Crystals. An Application of the Dynamic ADI Method", UCRL-92134
4. J. F. Nye, Physical Properties of Crystals, Clarendon Press, Oxford (1957).
5. S. G. Lekhnitskii, Theory of Elasticity of an Anisotropic Elastic Body, Holden-Day, Inc., San Francisco (1963).
6. A. B. Shapiro, "A Finite Element Heat Conduction Code for Analyzing 2-D Solids", UCID-20045 (March, 1984), Lawrence Livermore National Laboratory, Livermore, CA.
7. Standards on Piezoelectric Crystals, Proc. Institute of Radio Engineers, 37, 1378-95 (1949).
8. J. O. Hallquist, "A Vectorized, Implicit Finite Deformation, Finite Element Code for Analyzing the Static and Dynamic Response of 2-D Solids", UCID-19677 (Feb., 1983), Lawrence Livermore National Laboratory, Livermore, CA.